

A MODEL TO ESTIMATE EFFECTIVE EMITTANCES AND ABSORPTANCES

Victor F. Roriz¹, Rosana M. Caram² and Maurício Roriz¹

¹ Unicamp - Universidade Estadual de Campinas, Campinas (Brasil)

² EESC-USP - Universidade de São Paulo, São Carlos (Brasil)

1. Abstract

Typical bumps and hollows at the buildings surfaces, in roughness scale or like ripples on a tile, are obstacles that can significantly modify the behavior of these surfaces, in relation to the radiative flows. These flows are different that occurs in a perfectly smooth and flat surface. Therefore, the usual calculation procedures, which adopt the simplification that all surfaces of a construction are perfect plans, should apply corrections in the radiative properties. The absorptances and emittance resulting from these corrections could be called effective.

This paper presents a simple method developed to evaluate these influences and exemplifies the importance of such aspects, presenting results of simulations developed in the EnergyPlus for a simple geometry building, over 1 year in the city of Brasilia. Adopting effective absorptances and emittance, simulation results show differences above 2.5 ° C in the internal air temperature, compared to those obtained ignoring the influences that the ripples of the tiles have on radiant flows. Considering the use of air conditioners, this could represent more than 20% variation in a energy consumption estimate.

Keywords: absorptivity, emissivity, effective emittances, effective absorptances.




2. Introduction

The proper evaluation of the thermal properties of a surface is essential for a good correlation between theoretical models and reality. However, in many cases the terminology adopted for these properties is not standardized and the differences on the concepts ignored or neglected.

For this study, it was adopted the concepts that absorptivity and emissivity are properties of materials, while absorptances and emittance are surface characteristics, being influenced not only by the material they are made of, but also by its geometry and finish. For perfectly flat and smooth surfaces, these concepts are the same, but the prominences and hollows (undulations or roughness), present in the construction surfaces create shadows and reflections which affect the energy flow.

Many researchers have noticed the influence of shape and surface roughness on their radiative properties. Berdahl and Bretz (1997) performed tests on white coating of tiles and verified that a rough surface had a reflectance 25% lower than a flat one. Seker and Tavil (1996) and Barbirato et al (2000) also verified a reduction in the reflectance when the roughness was increased. Marchetti, Boudenne and Candau (2008), measured the effective emittance (ε_e) of paint with 3 different roughness, obtaining the results showed in Table 1.

Tab. 1: Effect of roughness on effective emittance. (adapt from: MARCHETTI, BOUDENNE E CANDAU, 2008).

Aluminium paint on a smooth surface	Aluminium paint on a slightly rough surface	Aluminium paint on a very rough surface
		
$\varepsilon_e = 0.34$	$\varepsilon_e = 0.42$	$\varepsilon_e = 0.69$

International standards for measuring emissivity, such as ASTM C1371 (2004) and JIS A1423 (1983) require the samples under analysis to be smooth and flat. In the same way, ASTM C1549 (2009) has the same requirement for the measurement of reflectance.

Sparrow and Jonsson (1963), calculate the effects caused in the radiative properties for some surfaces. Their deduction, however, refers to specific geometries, been applying only to particular cases.

This paper presents a simplified model for calculating the effective radiative properties of surfaces, applicable to any geometry. The results of applying this method are compared to those obtained by Sparrow and Jonsson (1963). Its presents an experimental model that demonstrates the effects of the phenomenon. The significance of the observance of such issues is demonstrated through computer simulations using EnergyPlus (DOE, 2010).

In the evaluation of heat fluxes and energy efficiency of a building, the processes mentioned here may have great relevance. For example, for roofs, depending on their shapes, a tile may have different thermal behaviour from others, even if made of the same material and received the same painting, etc. In the case of walls, the adoption of a texture could have an influence on their radiative behaviour and, consequently, on their surface temperatures.

3. Theoretical model

Consider the surface 1 presented in Figure 1 as an isothermal, gray and diffuse surface (radiation properties are independent of wavelength and direction), which emits heat to their surroundings (surface 2).

If all the energy emitted by surface 1 (E) is represented as coming from a single point (P_0), a portion of it may be emitted to the outside (vector \vec{A} , Eq. 1) and a second portion (vector \vec{B} , Eq.2) towards the surface itself.

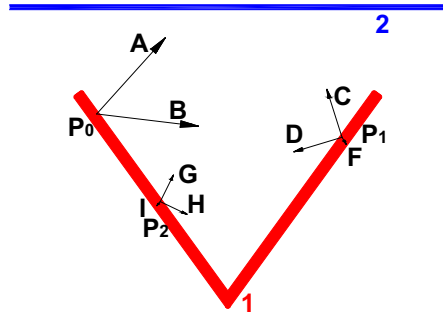


Fig. 1: Energy emitted by concave surface (1) to its surroundings (2)

Equations 1 and 2 use the concept of view factor (FF). The view factor (FF_{12}) of the surface 1 relative to the surface 2, can be defined as the ratio between the portion of radiant energy that comes out of 1 and is intercepted by 2, divided by all the radiant energy emitted by 1. By the same principle, FF_{11} refers to the portion of energy emitted by 1 and is intercepted by surface 1 itself.

$$\vec{A} = E.FF_{12} \text{ (eq. 1)}$$

$$\vec{B} = E.FF_{11} \text{ (eq. 2)}$$

Considering that the part represented by \vec{B} strike a point (P_1) of surface 1, a fraction of \vec{B} , which will be called \vec{C} , will also be reflected to the outside, adding to the vector \vec{A} , while a part \vec{D} will be reflected over the surface 1 again and a portion \vec{F} will be absorbed by surface 1.

Therefore, it is possible to consider three alternatives. In the first, the energy really leaves the surface 1 and reaches surface 2. In the second, the energy comes out of 1 and return to 1. In the third, the energy is absorbed by surface 1. Table 2 summarizes these hypotheses.

Tab. 2: Energy emitted by surface 1

REACHES 2	RETURN TO 1	ABSORBED BY 1
$\bar{A} = E.FF_{12}$	$\bar{B} = E.FF_{11}$	-
$\bar{C} = E.FF_{11} \cdot \rho \cdot FF_{12}$	$\bar{D} = E.FF_{11}^2 \cdot \rho$	$\bar{F} = E.FF_{11} \cdot \alpha$
$\bar{G} = E.FF_{11}^2 \cdot \rho^2 \cdot FF_{12}$	$\bar{H} = E.FF_{11}^3 \cdot \rho^2$	$\bar{I} = E.FF_{11}^2 \cdot \rho \cdot \alpha$

The portion of E that is really emitted to 2 (Ee), can then be calculated by the series:

$$E_e = \bar{A} + \bar{C} + \bar{G} + \dots \text{ (eq. 3)}$$

Therefore:

$$E_e = E.FF_{12} + E.FF_{11} \cdot \rho \cdot FF_{12} + E.FF_{11}^2 \cdot \rho^2 \cdot FF_{12} + \dots \text{ (eq. 4)}$$

By solving 4 is obtained:

$$E_e = \frac{E.FF_{12}}{1 - (FF_{11} \cdot \rho)} \text{ (eq. 5)}$$

Considering the surface of study as a cavity, as exemplified by the surface S1 with area A₁ in Figure 2, and its surroundings as a plan that limits this cavity (surface S2 with area A₂ in Figure 2), it is possible to consider the equation 6 and, by the equation 7, calculate the view factors between the surface and surroundings (Incropera and DeWitt, 1996).

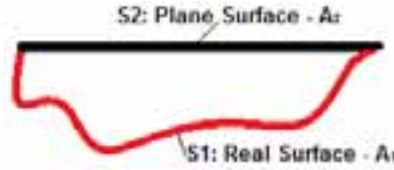


Fig. 2: Cut of a cavity

$$FF_{11} = 1 - FF_{12} \text{ (eq. 6)}$$

$$FF_{12} = \left(\frac{A_2}{A_1} \right) \text{ (eq. 7)}$$

The energy that really leaves the cavity S1, intersects the surface S2 and can be calculated by equation 8 (from 5 and 7).

$$E_e = \frac{E.FF_{12}}{1 - \rho_1 + FF_{12} \cdot \rho_1} \text{ (eq. 8)}$$

The emittance definition is:

$$\varepsilon = \frac{E}{E_{CN}} \text{ (eq. 9)}$$

Where:

$$E = A_1 \cdot \varepsilon_1 \cdot \sigma \cdot T_1^4 \text{ (eq. 10)}$$

$$E_{CN} = A_2 \cdot \sigma \cdot T_1^4 \text{ (eq. 11)}$$

Applying (8) and (11) in (9):

$$\varepsilon_e = \frac{E \cdot FF_{12}}{1 - \rho_1 + FF_{12} \cdot \rho_1} \cdot \frac{A_1}{A_2 \cdot \sigma \cdot T_1^4} \quad (\text{eq. 12})$$

From (10) and (12):

$$\varepsilon_e = \frac{\varepsilon_1 \cdot FF_{12}}{1 - \rho_1 + FF_{12} \cdot \rho_1} \cdot \frac{A_1}{A_2} \quad (\text{eq. 13})$$

Applying (7) in (13):

$$\varepsilon_e = \frac{\varepsilon_1}{1 - \rho_1 + FF_{12} \cdot \rho_1} \quad (\text{eq. 14})$$

Considering the surface as opaque, gray and diffuse, it comes from Kirchhoff's law:

$$\varepsilon = \alpha = 1 - \rho \quad (\text{eq. 15})$$

Therefore:

$$\varepsilon_e = \frac{\varepsilon_1}{\varepsilon_1 + FF_{12} - \varepsilon_1 FF_{12}} \quad (\text{eq. 16})$$

Or, by equation 7:

$$\varepsilon_e = \frac{\varepsilon_1 \cdot A_1}{A_2 - \varepsilon_1 \cdot A_2 + \varepsilon_1 \cdot A_1} \quad (\text{eq. 17})$$

Figure 3 shows the result of applying equation (17) to calculate the effect of the shape on the effective emittance. It is possible to see in this picture, that the reduction of the ratio between the areas A_1 and A_2 , indicated by the reduction of FF_{12} (see equation 7), implies in the increase of the effective emittance of the theoretical surface (surface S2 in Figure 2).

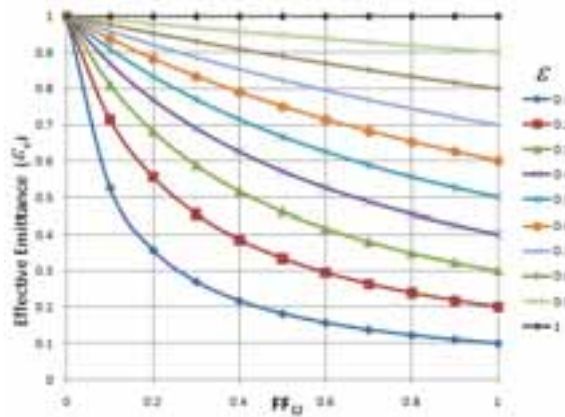


Fig. 3: Shape effect on the effective emittance

Similarly, for the absorptance, it is possible to develop a line of thought with the same principle. The absorbed energy (E_a), calculated as the sum of n portions absorbed, product of n-1 inter-reflections, can be obtained by the following equation (considering an irradiance I).

$$E_a = \alpha_e \cdot I = \alpha_1 \cdot I + (\alpha_1 \cdot FF_{11} \cdot \rho_1 \cdot I) + (\alpha_1 \cdot FF_{11}^2 \cdot \rho_1^2 \cdot I) + \dots \quad (\text{eq. 18})$$

$$E_a = \alpha_e \cdot I = \sum_{i=0}^n \alpha_1 \cdot FF_{11}^i \cdot \rho_1^i \cdot I \quad (\text{eq. 19})$$

The equation 18 can be obtained following this line of thought. If radiation strikes a diffuse surface, it will absorb the first part of the right side of the equation ($\alpha_1 \cdot I$). The energy not absorbed ($\rho_1 \cdot I$) would be reflected. And part of this reflection re-strike the surface ($FF_{11} \cdot \rho_1 \cdot I$). From this energy, the second part of the right side

of equation 17 would be absorbed ($\alpha_1 \cdot FF_{11} \cdot \rho_1 \cdot I$). Continuing, all parts of the equation 18 would be added.

Solving the equation 19 series :

$$\alpha_e = \frac{\alpha_1}{1 - (FF_{11} \cdot \rho_1)} \quad (\text{eq. 20})$$

Considering an opaque surface:

$$\alpha + \rho = 1 \quad (\text{eq. 21})$$

$$\alpha_e = \frac{\alpha_1}{1 - FF_{11} + FF_{11} \cdot \alpha_1} \quad (\text{eq. 22})$$

Or, from (6):

$$\alpha_e = \frac{\alpha_1 \cdot A_1}{A_2 - \alpha_1 \cdot A_2 + \alpha_1 \cdot A_1} \quad (\text{eq. 23})$$

Therefore, using equations 17 and 23 it is possible to calculate the values of effective emittance and absorptances, which may significantly differ from the values valid for perfectly smooth bodies, usually adopted in the heat flow calculations. The increase in absorptance caused by ripples ($\Delta\alpha$) can be calculated by equation 24 or 25 and is shown in Figure 4.

$$\Delta\alpha = \alpha_e - \alpha_1 \quad (\text{eq. 24})$$

$$\Delta\alpha = \frac{\alpha_1}{1 - FF_{11} + FF_{11} \cdot \alpha_1} - \alpha_1 \quad (\text{eq. 25})$$

From equation 25 it is possible to derive an equation for the maximum difference between the effective surface absorptance and their material absorptivity. The result of this operation is presented in equation 26.

$$\Delta\alpha_{\max} = 1 - 2 \cdot \alpha_1 \quad (\text{eq. 26})$$

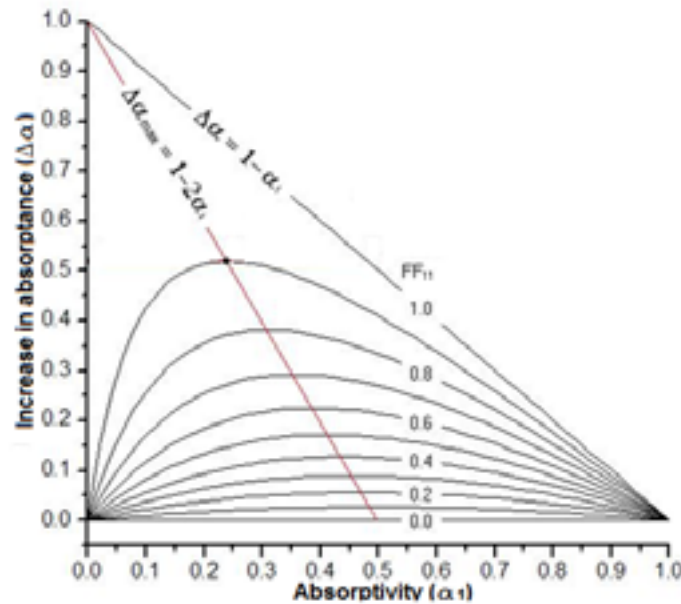


Fig. 4: Absorptance increase by shape effect

Admitting that the surface of interest is gray and diffuse, the energy is reflected in all directions (even over itself) with the same intensity in a hemispherical pattern (Figure 5), regardless of the incident radiation. In this case, the model used to develop the equation 23 is applicable to directional or non-directional radiation, and to any waveband. Therefore, this development could be applied to the spectrum of solar radiation

striking a building surface, whose high amount of energy can cause significant impacts on the buildings thermal flows.

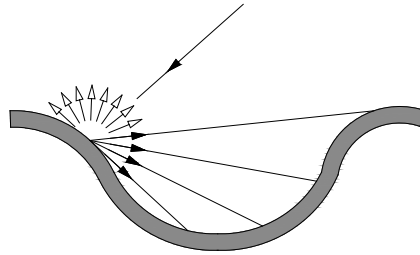


Fig. 5: Reflection of a diffuse surface

Sparrow and Jonsson [1963] developed precise models for evaluating this effect, however, their models are based on integrations of specific geometries studied and is therefore applicable only to themselves. Comparing results presented by Sparrow and Cess [1978] to those calculated by equation 16 to rectangular grooves is obtained the curves presented in Figure 6. In the model proposed by Sparrow the variation in radiosity between the surface points is considered. In the case of the rectangular groove (Figure 6), for example, the proximity of the opening would mean higher radiosities than in deeper points, implying also in a limit to the cavity effect. On the other hand, the model proposed in this paper considers that all points on the surface have the same behaviour. To spherical cavities, the solutions are identical, while for the rectangular grooves, the approximation is acceptable up to a ratio L/h of about 1.5 as shown in Figure 6. These limits satisfy most of the components of the building. Apart from this, the use of equation 17 has the advantages of its simplicity and its applicability to any form.

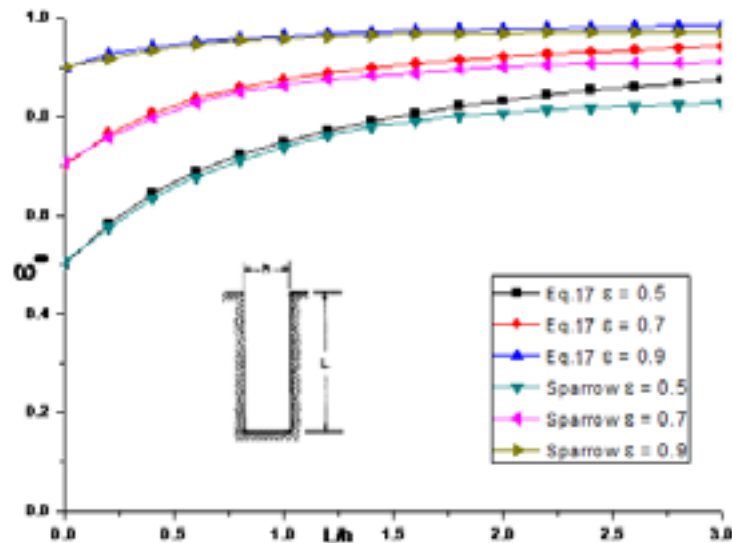


Fig. 6: Comparison of results of equation 17 to the model presented by Sparrow and Cess [1978]

4. Experiment

To illustrate the phenomena discussed here, a simple experiment was done. It consisted in monitoring the surface temperatures of four samples, built with the same mass and the same materials, but with different view factors, in an environment with controlled temperature and rarefied atmosphere.

It was compared the velocities of change in temperature of the samples, when submitted to sudden temperature changes of the environment in which they were. Correlation was found between the shapes of the samples and the respective differences in the rate of that temperature change. Figure 7 shows a schematic section of the experiment. In a vacuum chamber, a vacuum pump created a rarefied atmosphere in order to

minimize possible heat flows by convection.

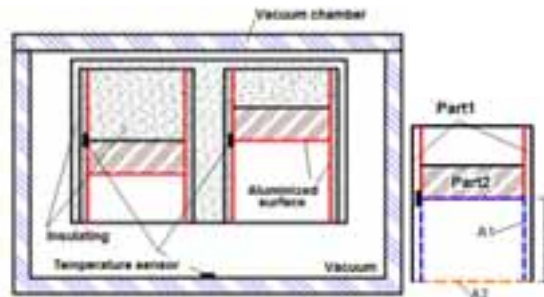


Fig. 7: Schematic section of the experimental apparatus and detail of one sample

Samples had bottom and sides covered with expanded polypropylene, minimizing other heat fluxes and enabling the record of the effects caused only by heat exchange by long wave radiation, between the samples and the chamber. Figure 8 shows the sample set and the system already prepared for the experiment. A pressure cooker was adapted as a vacuum chamber because it is airtight, opaque, made of aluminum (high conductivity), with polished surfaces (low emissivity) and convenient size, providing adequate conditions for the experiment.

The experimental procedure consisted in causing abrupt changes in the set temperature by submerging the vacuum chamber in iced or boiling water and recording the changes at the sample's temperatures over time.



Fig. 8: Vacuum chamber and the set of samples

Figures 9-11 show the temperatures recorded in an experiment, highlighting the periods of sudden cooling (Det. 1) and heating (Det. 2).

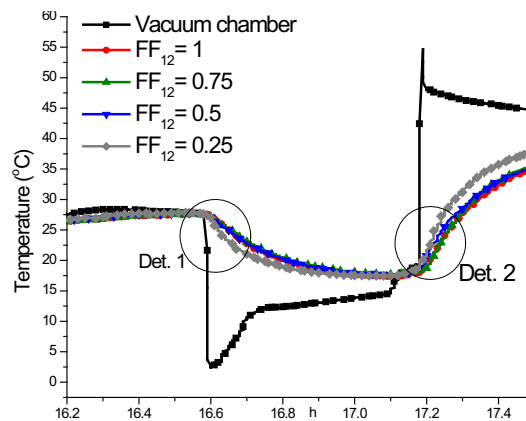


Fig. 9: Recorded temperatures

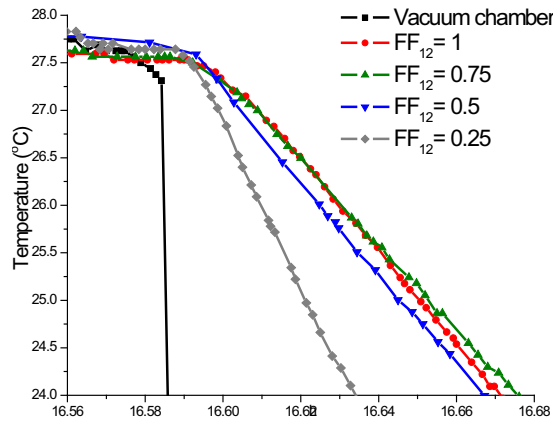


Fig. 10: Cooling period (Det. 1 in fig.9).

It is observed in Figures 9 and 10, that the sample with form factor of 0.25 is the one which more closely follows the temperature change of the chamber, followed by the sample which form factor of 0.5 and then by the factor form 0.75 and 1, between which there is practically no difference in temperatures.

Considering that the samples have the same composition and conditions, the explanation for this behavior is the greatest flow of heat by radiation between the camera and the sample that has the smallest form factor (larger exposed area), while the flow is lower for samples in which form factors are higher. In the cooling period (Fig. 10), the temperatures of the samples are higher than the surface of the chamber and thus the different behavior between the samples indicates differences between their effective emittance.

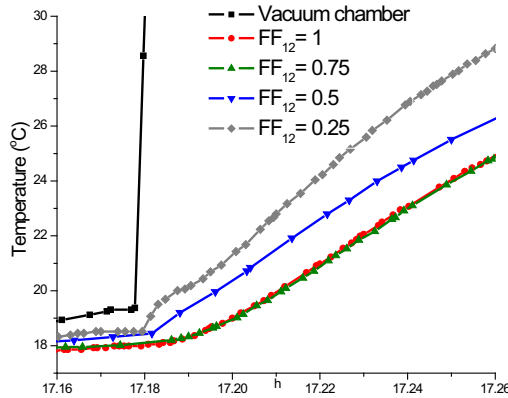


Fig. 11: Heating period (Det. 2 in fig.9).

During heating (Fig. 11), this process is reversed, prevailing the differences among effective absorptances. The same behavior could be expected in any case where the surface of interest can be admitted as gray and diffuse, like most of the surfaces of a construction.

5. Energy flux

According to Incropera e Dewitt (1996), the heat flux by radiation in a cavity formed by two gray and diffuse surfaces could be calculated by equation 27, whereas the equation 28 present the energy emitted by a flat surface to its surroundings.

$$q_{12} = \frac{\sigma(T_1^4 - T_2^4)}{\frac{1-\varepsilon_1}{\varepsilon_1 \cdot A_1} + \frac{1}{A_1 \cdot FF_{12}} + \frac{1-\varepsilon_2}{\varepsilon_2 \cdot A_2}} \quad (\text{eq. 27})$$

$$q_{12} = \sigma \cdot \varepsilon_e \cdot A_2 \cdot (T_1^4 - T_2^4) \quad (\text{eq. 28})$$

Taking tabulated values (Incropera and DeWitt, 1996) for the emissivity of the samples in 0.05 and the emissivity of the surface of the pressure vessel at 0.3, is possible to calculate by the equations 17, 27 and 28, the energy flows during the period recorded in experiment. Similarly, using the values proposed by Sparrow and Cess is possible to estimate these flows. Figure 12 compares the results obtained from equation 17 to these two other methods.

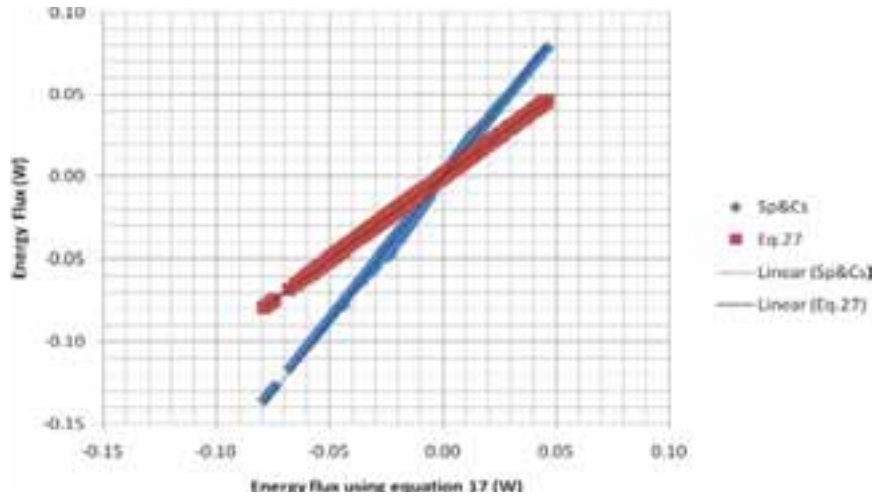


Fig. 12: Energy flux comparative

6. Simulation

To demonstrate the importance of such aspects, simulations have been made on the software EnergyPlus (DOE, 2010) for two buildings (Zone 1 and 2) of simple geometry (Fig. 13), submitted to the climate of the city of Brasilia (DF), Brazilian capital.



Fig. 13: Geometry of simulated environments (north facade).

The only difference between the two buildings was due to the radiative properties (emittance and absorptance) of their covering. In Zone1, it was assumed that the absorptances were equal to the absorptivity and emittance equal to the emissivity, as a perfectly smooth and flat surface. For Zone 2, it was considered the corrections proposed by equations 17 and 23, and covering composed of tiles as shown in figure 14, from where, by the equation 6, we obtain $FF_{12} = 0.65$. The physical properties adopted for materials and surfaces were presented in Table 3.

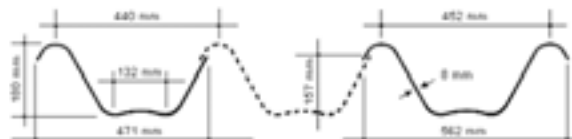


Fig. 14: Adopted tiles.

Tab. 3: Surface properties

MATERIAL	THICKNESS (m)	CONDUCTIVITY (W/m.K)	SPECIFIC HEAT (J / kg K)
Walls	0.1	0.75	1500
Floor	0.05	1.7	2300
Tile Zone 1	0.006	1.7	2300
Tile Zone 2	0.006	1.7	2300
MATERIAL	DENSITY (kg/m ³)	EMITTANCE	ABSORPTANCE
Walls	960	0.9	0.4
Floor	960	0.9	0.4
Tile Zone 1	960	0.9	0.6
Tile Zone 2	960	0.933	0.698

For both zones parallelepipeds-shaped buildings were considered with 6 x 9 x 2.8 (m), and 4m2 shaded windows facing north, without heat flows to the ground. It was adopted 10 cm ceramic brick walls and floor with 5 cm of concrete. It remained a constant ventilation rate of 5 changes per hour and internal heat sources corresponding to people and equipment, as shown in Figure 15.

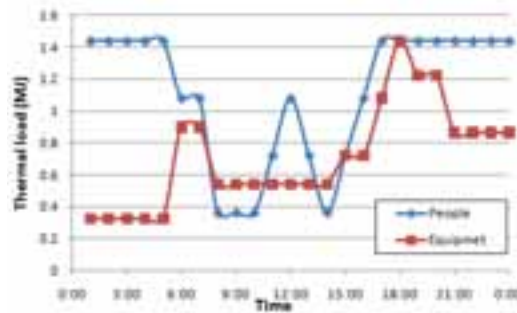


Fig. 15: Thermal load.

The EPW climate file of Brasilia (DOE, 2010) was simulated for an entire year, resulting in a maximum difference in temperature (TZone2-TZone1) of 1.65 °C. Figure 16 illustrates the obtained results.

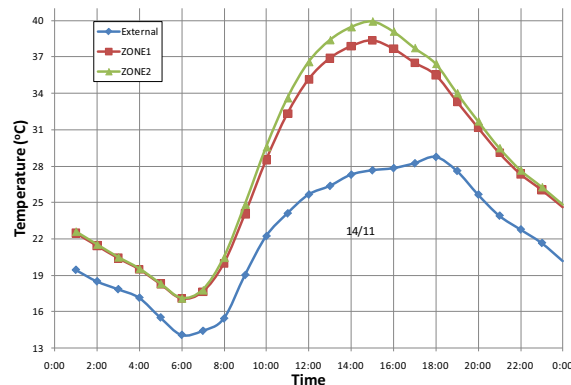


Fig. 16: Temperatures obtained in the simulation sample for the day 14/11.

It is known that many parameters may affect this kind of simulation and could be changed in this study. For example, the simple reduction of the ventilation rate from 5 to 1 changes per hour increases the maximum difference in temperatures between zones (TZone2-TZone1) to 2.83 °C. Notice that the latest Brazilian technical standard on buildings performance (NBR 15575, ABNT, 2008) indicates that the simulations must adopt 1 change per hour. By changing the wall material to a less conductive one, such as oak wood (0.15

W/m.K, 1424 J / kg K) and keeping the other original parameters, the maximum difference in temperatures between zones (TZone2-TZone1) increases to 1.89 °C.

To test the impact of these aspects in energy consumption it was simulated the use of ideal air conditioners in both zones. It was adopted a limit (set point) of 24 °C for internal temperature and the sums of consumption needed to maintain the internal temperatures below this value, throughout the entire year, were compared.

The internal temperatures obtained and their cooling thermal loads are illustrated in Figure 17. For Zone1 the sum of the annual load was 104.4 GJ, while for Zone2 this value was 120.1 GJ, thus presenting a 15% increase over consumption seen in Zone1. For the case mentioned in which the ventilation rate is reduced for one change per hour, this difference greatly increases, reaching 30%.

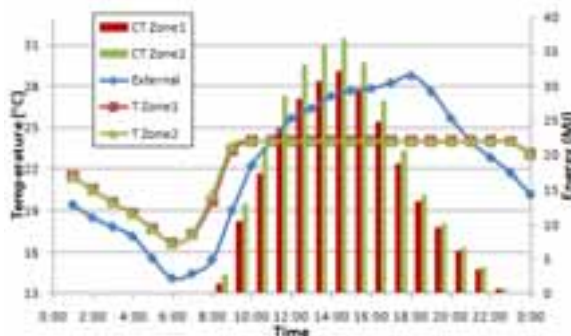


Fig. 17: Temperatures and thermal loads obtained in the simulation. Example for the climatic conditions of the day 14/11.

7. CONCLUSION

The studied variables present high relevance for evaluations of thermal comfort and energy efficiency of built environments.

The simulations revealed considerable differences in the air temperatures and energy consumption estimative among the models that consider or not, the corrections proposed for the effective properties of the surfaces. It was evidenced that the differences between surface properties and properties of materials cannot be neglected at the risk of major inaccuracies in the calculations of heat flows.

For the typical surfaces found in buildings, the simplified model described in this paper correlates well with the classical model developed by Sparrow and Jonsson, having the advantage of being simpler and not restricted to specific forms.

8. REFERENCES

- ABNT – Associação Brasileira De Normas Técnicas NBR 15 575 – Edifícios Habitacionais De Até Cinco Pavimentos – Desempenho. Rio de Janeiro, 2008
- ASTM C 1371-04. (2004). Standard Test Method for Determination of Emittance of Materials Near Room Temperature Using Portable Emissometers.
- ASTM C1549 – 09 (2009) Standard Test Method for Determination of Solar Reflectance Near Ambient Temperature Using a Portable Solar Reflectometer
- Barbirato, G. M., Silva, C. A., Machado, I. B., , Oiticica, M. L. (2000). Refletância de cores em superfícies construtivas. Anais do VIII Encontro Nacional de Tecnologia do Ambiente Construído ENTAC. Salvador.
- Berdahl, P., Bretz, S. E. (1997). Preliminary Survey of the solar reflectance of cool roofing materials. Energy and Buildings, 25.
- DOE – U. S. Department Of Energy. Building Energy Software Tools Directory <www.eere.energy.gov/buildings/tools_directory/alpha_list.cfm>

Incropera, F. P., Dewitt, D. F. (1996). Fundamentals of heat and mass transfer (4. ed.). New York. John Wiley and Sons.

JIS A 1423. (1983). Simplified test method for emissivity by infrared radio meter.

Marchetti, Boudenne and Candau (2008). Analysis of the radiative behavior of road materials: Principles and measurements of infrared emissivity. Bulletin des Laboratoires des Ponts et Chaussées, 272 (2008) pp 45-55.

Seker, D. Z., Tavit, A. Ü. (1996). Evaluation of exterior building surface roughness degrees by photogrammetric methods. Building and Environment , 31, pp. 393-398.

Sparrow, E. M., , Cess, R. D. (1978). Radiation Heat Transfer. London: Hemisphere Publishing Corp.

Sparrow, E., Jonsson, V. (1963). Radiant Emission Characteristics of Diffuse Conical Cavities. Journal of the Optical Society of America , 53, pp. 816-821.

9. ACKNOWLEDGEMENTS

The authors are thankful to FAPESP (Fundação de Amparo à Pesquisa do Estado de São Paulo) for the doctorate scholarship which allowed the development of this research.